



CHORUS

This is the accepted manuscript made available via CHORUS. The article has been published as:

Examination whether heavy quarks carry information on the early-time coupling of the quark-gluon plasma

A. M. Adare, M. P. McCumber, J. L. Nagle, and P. Romatschke

Phys. Rev. C **90**, 024911 — Published 26 August 2014

DOI: [10.1103/PhysRevC.90.024911](https://doi.org/10.1103/PhysRevC.90.024911)

Do Heavy Quarks Carry Information on the Early-Time Coupling of the Quark-Gluon Plasma?

A. M. Adare,¹ M. P. McCumber,² J. L. Nagle,¹ and P. Romatschke¹

¹University of Colorado at Boulder

²Los Alamos National Laboratory

(Dated: July 30, 2014)

The redistribution in momentum space of heavy quarks via their interactions in the quark-gluon plasma is an excellent probe of the heavy quark coupling strength to the medium. We utilize a Monte Carlo Langevin calculation for tracking heavy quark - antiquark pairs embedded in a viscous hydrodynamic space-time evolution. We find that the nuclear modification factor (R_{AA}) for charm quarks is relatively insensitive to the coupling to the quark-gluon plasma at early times where the highest temperatures are achieved. In contrast the azimuthal angular correlation of charm and anticharm quarks is extremely sensitive to the early time evolution. For beauty quarks the situation is reversed in terms of sensitivity. This work identifies the kinematic distributions of the heavy quarks with the greatest sensitivity, and must be followed by tests of whether they survive hadronization, in particular if recombination is dominant.

PACS numbers: 25.75.Dw

High energy heavy ion collisions at the Relativistic Heavy Ion Collider (RHIC) and the Large Hadron Collider (LHC) produce nuclear matter at sufficiently high temperatures to create droplets of the quark-gluon plasma (QGP). Even at the highest temperatures achieved, thermal production of heavy quark-antiquark pairs is suppressed and the $c\bar{c}$ and $b\bar{b}$ pairs are produced primarily at the earliest times in large momentum transfer reactions between incoming partons within the incident nuclei. Due to flavor conservation of the strong interaction, the heavy quarks emerge from the QGP within a charm or beauty hadron. Heavy quarks therefore act as “tracers” that record the evolution of the QGP through thermalization, hydrodynamic expansion, and hadronization, even if the QGP itself has no long-lived quasiparticles [1].

It was proposed in Ref. [2] that the interactions of heavy quarks have a weaker effective coupling to the medium by a “dead cone” effect that reduces the phase space for radiative energy loss. However, initial experimental results were consistent with charm quarks following the flow of the underlying quark-gluon plasma [3]. Subsequently, the degree of thermalization was studied within a Langevin approach by Moore and Teaney [4]. Reasonable agreement with the suppression and elliptic flow of heavy quark mesons measured via semi-leptonic decay electrons is achieved with a diffusion rate requiring the shear viscosity over entropy density (η/s) to lie within a factor of two of the conjectured $1/4\pi$ limit [5]. Numerous works have employed similar Langevin calculations with different assumptions about the heavy quark-medium coupling and the underlying quark-gluon plasma space-time evolution [6–11].

A preliminary measurement of the D meson R_{AA} in 0-10% central $Au + Au$ collisions at $\sqrt{s_{NN}} = 200$ GeV is shown in Figure 1 [12]. The data are in close agree-

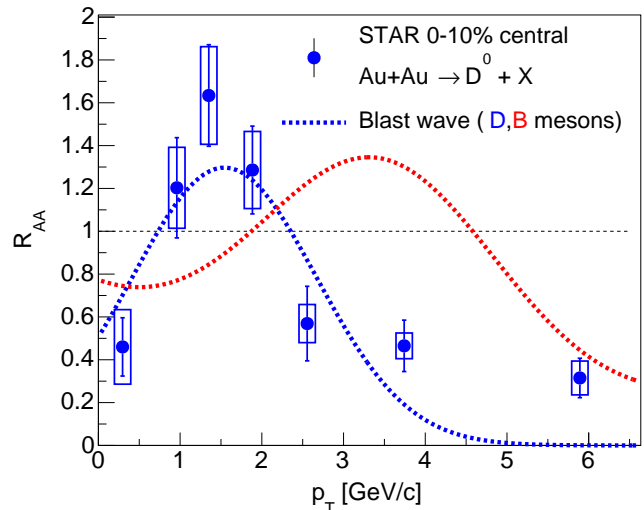


FIG. 1: R_{AA} of D^0 mesons in 0-10% central $Au + Au$ at $\sqrt{s_{NN}} = 200$ GeV compared with blast-wave calculations for D and B mesons and a PYTHIA $p + p$ baseline reference.

ment with a blast wave prediction from Ref. [3] up to $p_T \approx 3.5$ GeV/ c . The calculation utilizes PYTHIA for the $p + p$ baseline, and for $Au+Au$ a linear boost profile blast wave model constrained by π , K , and p transverse momentum distributions. In the blast wave model, an outward push from radial flow leads to a trend of suppression for $p_T < 1$ GeV/ c , followed by an enhancement for $p_T \approx 1 - 2.2$ GeV/ c . Since the radial flow boost available within the model is limited, suppression occurs for $p_T > 2.2$ GeV/ c . At higher momenta, the heavy quarks increasingly deviate from thermal equilibrium, and the blast wave model and the data are expected to diverge. In this paper, we aim to understand the full time evolution of the charm and beauty quark distributions in space and momentum, and to test whether the blast wave final-

state parametrization is reproducible at the quark level.

We have implemented a Monte Carlo Langevin calculation to trace the diffusion and drag of individual heavy quarks. We have tested the numerical algorithm against the control thermalization tests in Ref. [8] and obtain identical results. The transverse momentum distribution of the initial heavy quarks are selected from the following equation:

$$\frac{1}{p_T} \frac{dN}{dp_T} \propto \frac{1}{(p_T^2 + \Lambda^2)^\alpha} \quad (1)$$

where $\alpha = 3.9$ (4.9) and $\Lambda = 2.1$ (7.5) for charm (beauty) quarks, following Ref. [13]. We then generate initial conditions by averaging over central Au+Au collisions at $\sqrt{s_{NN}} = 200$ GeV with a Monte Carlo Glauber code [14], where each event is rotated into the axis of the participant plane. The event averaging ensures a smooth spatial configuration for numerical stability in the subsequent hydrodynamic evolution. The initial heavy quark-antiquark pair positions are sampled from this smooth distribution of binary collisions.

An initial transverse momentum k_T sampled randomly from $\mathcal{N}(k_T | \mu = 0, \sigma^2 = 1.0 \text{ GeV}/c)$ is added to the $c\bar{c}$ and $b\bar{b}$ pairs at their point of production, where \mathcal{N} is the normal distribution. We note that the effect of varying k_T has been studied in e.g. Ref. [9], and in the end such parameters must be constrained from $p+p$ and $p(d)+A$ experimental data. This k_T effect alone results in an enhancement of charm quarks at $p_T \approx 1 \text{ GeV}/c$ of approximately 10%.

We then run the viscous hydrodynamic code from Luzum and Romatschke [15, 16] to generate the space-time distribution of temperature T , energy density, and fluid velocities. The original code has been modified for new input and output formats. We then run individual heavy quark-antiquark pairs in time steps of 0.025 fm/c through the space-time background distribution, updating the 3-momentum information at each step according to the Langevin equation

$$\frac{d\mathbf{p}(t)}{dt} = -\eta_D(p) \mathbf{p}(t) + \boldsymbol{\xi}(t). \quad (2)$$

As a consequence of the fluctuation-dissipation theorem, all of the essential physical effects (scattering, viscous drag, and hydrodynamic boosts) are controlled by a single diffusion parameter D at the local temperature T of the thermal background. The viscous drag force $\eta_D(p) = T/(ED)$ describes the large-scale average motion of a particle with energy E , while ξ^i describes fluctuations in coordinate i about the average motion as follows:

$$\langle \xi^i(t) \xi^j(t') \rangle = \frac{2T^2}{D} \delta^{ij} \delta(t - t'), \quad \langle \xi^i(t) \rangle = 0. \quad (3)$$

This is implemented in the Langevin calculation by applying a momentum deflection Δp sampled at random

from $\mathcal{N}(\Delta p | \mu = 0, \sigma^2 = 2T^2/D\Delta t)$ at each time step Δt . We tested that increasing Δt by a factor of 10 does not change the results.

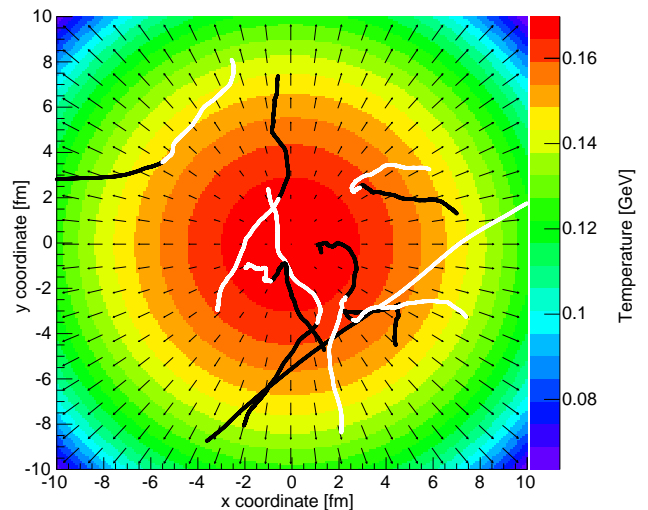


FIG. 2: Illustration of few $c\bar{c}$ pair trajectories in the expanding medium after 10 fm/c, with a diffusion parameter value of $D = 3/2\pi T$. The color scale shown in the right-side vertical axis indicates the temperature of the individual fluid cell and the small arrows indicate the direction and relative magnitude of the fluid cell velocities. The black and white paired thick lines are charm-anticharm quark trajectories from their initial common creation point up to the time 10 fm/c.

In principle, D depends on the momentum of the quark in the fluid rest frame. All the results shown here are calculated under the assumption that D is independent of momentum as done for example in Refs. [4, 13].

Figure 2 shows a visual record of the path traversed by a few typical charm-anticharm pairs. The nuclear modification of the c and b quark p_T distributions is plotted in Figure 3 for different “snapshots” during the evolution of the system. At the starting time of 1 fm/c, the R_{AA} is statistically consistent with one. Note that we have plotted the R_{AA} distributions relative to the result with just the initial k_T broadening so as to highlight only the change from the drag and diffusion in medium. During the first 7 fm/c, the R_{AA} rises at low p_T , and drops at higher p_T . After 7 fm/c, the trend reverses: R_{AA} moves downward at low p_T and increases at intermediate p_T , due to the strong radial flow velocities that have developed in the medium. Since the initial heavy-quark p_T distribution is much harder than the thermal distribution of the quark-gluon plasma, the Langevin drag term dominates over the diffusion term, pulling the c and b quarks to lower p_T . Given enough time in a static medium, the heavy quarks would eventually follow a thermal distribution with the medium temperature, as studied in [17]. It is notable, however, that the final R_{AA} remains above 1.0

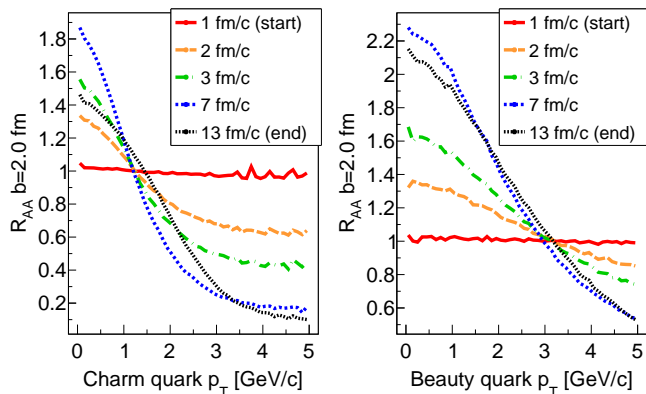


FIG. 3: Charm quark (left) and beauty quark R_{AA} (right) at various times during the hydrodynamic evolution.

at low transverse momentum, in contrast to the suppression seen in the D meson data and the blast wave result (Figure 1).

The initial hydrodynamic results were produced assuming a constant value of $\eta/s = 1/4\pi$ translated to the diffusion parameter using the relation

$$D(T) = \frac{\eta}{s} \frac{6}{T} \quad (4)$$

which is based on [5]. For full consistency, the hydrodynamic simulation should be modeled with a shear viscosity following the same relationship as that applied to the heavy quarks, but in order to isolate the effects of quark-medium interactions, the hydrodynamical model always uses a constant shear viscosity such that $\eta/s = 1/4\pi$ in all studies presented here.

We explore the dependence of R_{AA} on diffusion strength by running the calculation with a range of diffusion parameters D . We use the correspondence of Eq. 4 for η/s equaling various factors of $1/4\pi$, specifically $D = \{0.5, 1, 2, 4\} \times 3/(2\pi T)$. The final R_{AA} curve for each D value is shown in Figure 4 for c quarks (left) and b quarks (right). For charm quarks, the differences in R_{AA} for transverse momentum below 2.0 GeV/c are quite modest ($\pm 10\%$) despite an eight-fold variation of the diffusion parameter. Even if the diffusion is made to be extremely small by using, e.g. $D \times 2\pi T/3 = 0.01$ (not shown), R_{AA} remains above 1.0 at low p_T for both species.

The low- p_T charm quark R_{AA} is insensitive to the diffusion strength because the initial drag and the late-stage radial push tend to cancel one other. For beauty quarks, however, the low- p_T enhancement is dramatically increased as D is reduced, due to the downward redistribution in p_T . For the b quarks, the late-stage push is a weaker effect, leading to less cancellation against the early-stage energy loss.

The balancing of early and late-time effects and the lack of ability to achieve $R_{AA} < 1$ at low p_T led us to

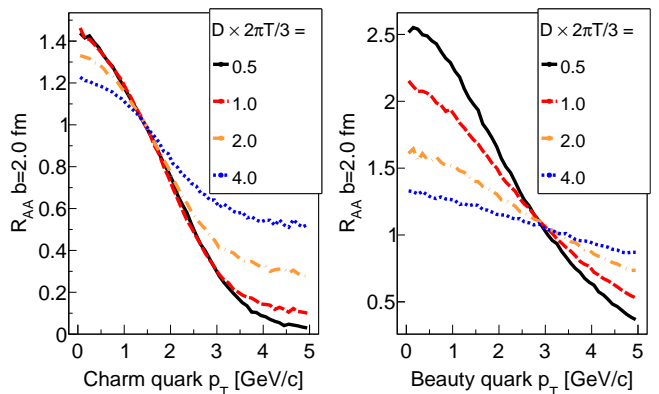


FIG. 4: Nuclear modification factor R_{AA} for charm quarks (left) and beauty quarks (right) at several values of the diffusion parameter D .

explore the temperature dependence of the diffusion parameter. If D increases at higher temperatures (e.g. η/s rises as a function of temperature above the quark-gluon plasma transition temperature), then the early-time drag will be weaker and the later time flow boost could result in a depletion at low p_T .

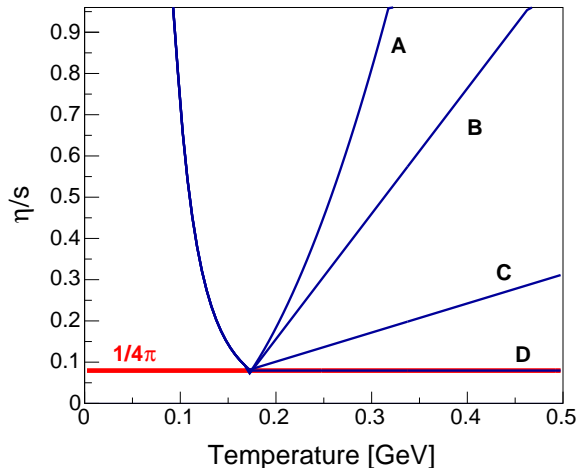


FIG. 5: Temperature dependence of η/s for a variety of scenarios.

We have considered four different η/s temperature dependence scenarios from Ref. [18] (Figure 5), which are converted to the diffusion parameter $D(T)$ using Eq. 4 for input to the Langevin calculation. We note that Eq. 4 is conjecture and the real constraint is on the temperature dependence $D(T)$. Scenarios B and C are motivated by recent bulk hydrodynamic fits to the data at RHIC and the LHC [19–22]. We note that the temperature dependence of the diffusion parameter from Ref. [4] was calculated perturbatively, and here we just phenomenologically parameterize the lower temperature ($T < 500$ MeV) dependence. The results from the four scenarios for the c and b

quark nuclear modification factor are shown in Figure 6.

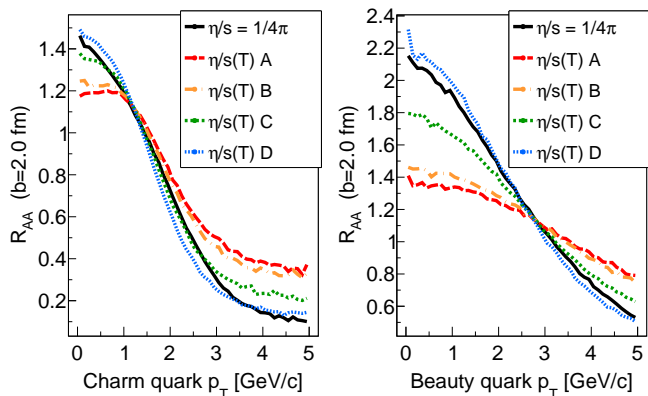


FIG. 6: Nuclear modification factors for charm quarks (left) and beauty quarks (right) for the set of $\eta/s(T)$ functions shown in Figure 5.

It is notable that none of the scenarios *A-D* lead to a depletion of charm quarks at low transverse momentum, despite the large variation of diffusion strength at high-temperature. This suggests that the strong R_{AA} “hump” in Figure 1 is not likely to be from quark-medium interactions alone. In the blast-wave model, the heavy quarks are distributed over the entire transverse plane such that a large fraction are positioned at large radii, where the late-stage hydrodynamic push is largest.

To demonstrate the dependence of nuclear modification on initial quark radial positions R , Figure 7 shows R_{AA} for charm quarks originating in several different R selections. Only when all charm quarks originate at

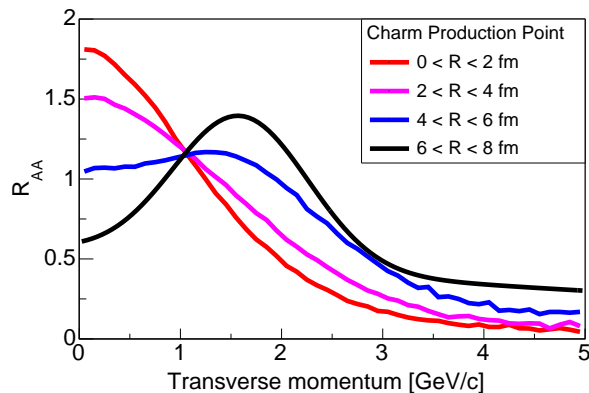


FIG. 7: R_{AA} for charm quarks produced within four different radial intervals using $D = 3/2\pi T$.

$R > 6$ fm does the Langevin charm R_{AA} qualitatively reproduce the shape found in Figure 1. Since most quarks originate within 4 fm of the medium centroid in any realistic central Au+Au model, the initial-state geometric configuration appears unlikely to play a large role in determining the shape of R_{AA} . It has been suggested that

pre-equilibrium radial flow may redistribute the heavy quarks outward and impart a significant radial velocity to the heavy quarks. We did study the effect of pre-equilibrium flow from Ref. [23] in our Langevin calculation, but did not observe any qualitative change to the results presented here.

Additionally, it is worthwhile to test whether these results are robust against the assumption that the diffusion parameter D is constant with momentum. We checked this by implementing a momentum dependent $D(p)$ following the results of Ref. [24] (Fig. 20, Potential 1 Th-Scheme) in which the relaxation rate decreases by about 50% over a momentum range of 0 to 4 GeV/c. As expected, the charm quark R_{AA} at higher p_T (≈ 4 -5 GeV/c) shows less suppression, since these higher momentum quarks are more weakly coupled. Although we observed modest changes to the lower p_T R_{AA} , the qualitative conclusions from the previous figures are unmodified by using a momentum-dependent diffusion parameter.

We note that in Figure 4 of Ref. [4] for the smallest diffusion parameter considered, the charm R_{AA} does turn down at low p_T , though never decreasing below one. Running our calculation also for $b = 6.5$ fm (midcentral) Au+Au and with identical parameters, we qualitatively reproduce these results. Despite smaller fluid velocities in more peripheral events, it is more likely for the charm quarks to be located near the surface of the medium.

To recapitulate, we have found that in central Au+Au events, no moderate value for the Langevin diffusion parameter, nor any realistic distribution of heavy quark initial positions, nor pre-equilibrium flow, is capable of producing the low- p_T heavy-quark R_{AA} values such as those observed for D mesons in Figure 1. It is possible that the low- p_T heavy-flavor meson R_{AA} is not primarily due to physics occurring at the partonic stage, but rather hadronic mechanisms such as recombination [25]. Various calculations of recombination (see for example Refs. [6, 26, 27]) are able to qualitatively reproduce the R_{AA} shape and further studies are needed to constrain this modeling and determine if the heavy quark information is washed out in the process.

We have seen that R_{AA} for charm quarks with $p_T < 2$ GeV/c does not reflect a strong dependence on the diffusion coefficient in the high-temperature regime. A quantity that is potentially more sensitive to early-time dynamics is the distribution in relative azimuth $\Delta\phi$ for heavy quark pairs, which has been studied previously in Refs. [11, 28–31].

In striking contrast to R_{AA} , the $c\bar{c}$ $\Delta\phi$ distributions shown in Figure 8 reflect a very strong sensitivity to variations in high-temperature diffusion. The left upper (lower) panel shows the results for charm-anticharm quark pairs with final $p_T > 0$ ($p_T > 2$) GeV/c. These results when mapped to a comparable coupling are qualitatively similar to those in Ref. [11]. The right panels show

the same quantity for beauty-antibeauty quark pairs. It is interesting to note that when comparing Scenarios A and D, the difference in the mean $\Delta\phi$ value is nearly the same 0.3 radians for both charm-anticharm and beauty-antibeauty pairs. However, while there is a significant decrease in the number of beauty pairs with $\Delta\phi \approx \pi$, the number of pairs re-directed along the same direction $\Delta\phi \approx 0$ remains small for any medium coupling scenario.

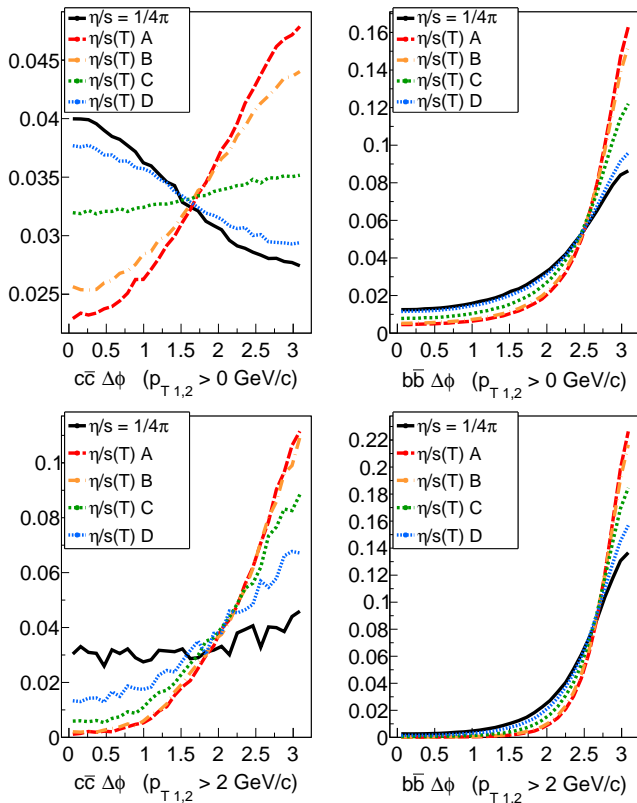


FIG. 8: $\Delta\phi$ distributions for charm quarks (left) and beauty quarks (right) for the set of $\eta/s(T)$ functions shown in Figure 5. The top row includes $q\bar{q}$ pairs at all momenta, and the bottom row includes $q\bar{q}$ pairs where both quarks have $p_T > 2$ GeV/c.

When D is large at high temperature, the $c\bar{c}$ angular correlation is peaked at $\Delta\phi = \pi$. This feature is expected for weak early-time quark-medium interactions, where the initial back-to-back kinematics are preserved. When D is small, the $c\bar{c}$ angular distribution exhibits a distinct near-side correlation. This is due to (a) strong initial scattering and drag that slows the quarks and destroys their initial opposing trajectories, and (b) the late-stage radial push that acts to collimate the quark-antiquark pairs – as seen for example in the top right quadrant in Figure 2. For the $b\bar{b}$ pairs, however, the initial energy loss is considerably smaller than for charm quarks at comparable momenta, as shown in Figure 4, thus retaining the away-side dominated azimuthal pair distribution.

In order to confirm that the azimuthal angle modifica-

tions are dominated by early time dynamics, we calculate the mean relative azimuthal angle between charm-anticharm quark pairs for each time step $\langle\delta\phi\rangle$. We then calculate the change in this quantity as a function of time in the medium evolution $d(\langle\delta\phi\rangle)/dt$. The results for all pairs in the four coupling scenarios are shown in Figure 9 (upper panel). The largest change in the angular correlation is at the earliest time and all scenarios collapse to the low rate of change at later times, as expected since all scenarios have the same coupling for $T < 170$ MeV/c. We have performed the same calculation for four fixed (i.e. temperature independent) values of η/s as shown in Figure 9 (lower panel). The results highlight that the large difference in coupling at late times has very little impact on the angular correlation. Also shown in both panels as solid points are the results of the integrated change over time $\Delta(\langle\delta\phi\rangle)$ for Scenario D (upper) and fixed $\eta/s = 1/4\pi$ (lower). The results are almost identical despite the large difference in coupling for $T < 170$ MeV/c as shown in Figure 5, again indicating sensitivity only to the early time dynamics.

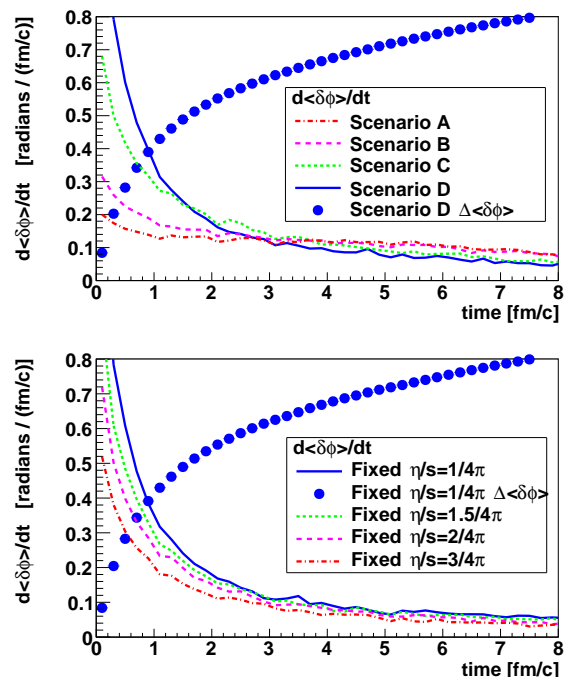


FIG. 9: Plotted is the change in the mean charm-anticharm quark azimuthal angle correlation as a function of time for the four $\eta/s(T)$ scenarios (upper) and for four fixed η/s value cases (lower). Also shown are the integrated change in the angle correlation for Scenario D (upper) and fixed $\eta/s = 1/4\pi$ (lower) which differ only by the coupling for $T < 170$ MeV/c.

In summary, the Monte Carlo Langevin framework, coupled with a time-dependent viscous hydrodynamic medium model, provides a useful tool for studying the space-time evolution of interactions between heavy

quarks and the thermal medium. Stochastic scattering and viscous drag lead to high- p_T suppression, as well as an enhancement of particles at intermediate p_T . However, late-stage hydrodynamic expansion is insufficient to cause $R_{AA} < 1$ for very low p_T heavy quarks when a realistic initial geometry is used. These calculations indicate that azimuthal correlations involving $c\bar{c}$ pairs are more sensitive to the diffusion strength than R_{AA} . In contrast, the heavier $b\bar{b}$ has significant sensitivity via the R_{AA} . Hadronization mechanisms, such as coalescence, may be relevant in explaining the low- p_T suppression observed in heavy-flavor mesons. Next steps include full modeling of hadronization effects and identifying the specific optimal experimental observables that reflect the underlying heavy quark final distributions.

We gratefully acknowledge useful discussions with Joerg Aichelin, Steffen Bass, Shanshan Cao, Matt Luzum, and Krishna Rajagopal. AMA and JLN acknowledge support from the United States Department of Energy Division of Nuclear Physics grant DE-FG02-00ER41152. PR acknowledges support from DOE award No. DE-SC0008027 and Sloan Award No. BR2012-038. MPM acknowledges support from the Los Alamos National Laboratory LDRD project 20120775PRD4.

-
- [1] Nuclear Science Advisory Committee Reports (2013), URL http://science.energy.gov/~media/np/nsac/pdf/20130201/2013_NSAC_Implementing_the_2007_Long_Range_Plan.pdf.
- [2] Y. L. Dokshitzer and D. Kharzeev, *Phys.Lett.* **B519**, 199 (2001).
- [3] S. Batsouli, S. Kelly, M. Gyulassy, and J. Nagle, *Phys.Lett.* **B557**, 26 (2003).
- [4] G. D. Moore and D. Teaney, *Phys.Rev.* **C71**, 064904 (2005).
- [5] A. Adare et al. (PHENIX Collaboration), *Phys.Rev.Lett.* **98**, 172301 (2007).
- [6] M. He, H. van Hees, P. B. Gossiaux, R. J. Fries, and R. Rapp (2013), 1305.1425.
- [7] S. Cao, G.-Y. Qin, S. A. Bass, and B. Mller, *Nuclear Physics A* **904905**, 653c (2013), ISSN 0375-9474, proceedings of the {XXIII} International Conference on Ultrarelativistic NucleusNucleus Collisions, URL <http://www.sciencedirect.com/science/article/pii/S0375947413002261>.
- [8] S. Cao, G.-Y. Qin, and S. A. Bass, *J.Phys.Conf.Ser.* **420**, 012022 (2013).
- [9] H.-j. Xu, X. Dong, L.-j. Ruan, Q. Wang, Z.-b. Xu, et al. (2013), 1305.7302.
- [10] Y. Akamatsu, T. Hatsuda, and T. Hirano, *Phys.Rev.* **C79**, 054907 (2009).
- [11] X. Zhu, N. Xu, and P. Zhuang, *Phys.Rev.Lett.* **100**, 152301 (2008).
- [12] D. Tlusty (STAR collaboration), *Nucl.Phys.A904-905* **2013**, 639c (2013).
- [13] S. Cao, G.-Y. Qin, and S. A. Bass (2012).
- [14] B. Alver, M. Baker, C. Loizides, and P. Steinberg (2008).
- [15] M. Luzum and P. Romatschke, *Phys. Rev. C* **78**, 034915 (2008), URL <http://link.aps.org/doi/10.1103/PhysRevC.78.034915>.
- [16] M. Luzum and P. Romatschke, *Phys. Rev. C* **79**, 039903 (2009), URL <http://link.aps.org/doi/10.1103/PhysRevC.79.039903>.
- [17] S. Cao and S. A. Bass, *Phys. Rev. C* **84**, 064902 (2011), URL <http://link.aps.org/doi/10.1103/PhysRevC.84.064902>.
- [18] C. Aidala, N. Ajitanand, Y. Akiba, Y. Akiba, R. Akimoto, et al. (2012), 1207.6378.
- [19] H. Song, S. A. Bass, U. Heinz, T. Hirano, and C. Shen, *Phys. Rev. C* **83**, 054910 (2011), URL <http://link.aps.org/doi/10.1103/PhysRevC.83.054910>.
- [20] H. Niemi, G. S. Denicol, P. Huovinen, E. Molnár, and D. H. Rischke, *Phys. Rev. Lett.* **106**, 212302 (2011), URL <http://link.aps.org/doi/10.1103/PhysRevLett.106.212302>.
- [21] C. Gale, S. Jeon, B. Schenke, P. Tribedy, and R. Venugopalan, *Phys. Rev. Lett.* **110**, 012302 (2013), URL <http://link.aps.org/doi/10.1103/PhysRevLett.110.012302>.
- [22] J. L. Nagle, I. G. Bearden, and W. A. Zajc, *New J.Phys.* **13**, 075004 (2011).
- [23] W. van der Schee, P. Romatschke, and S. Pratt, in preparation (2013).
- [24] F. Riek and R. Rapp, *Phys.Rev.* **C82**, 035201 (2010).
- [25] M. He, R. J. Fries, and R. Rapp, *Phys. Rev. Lett.* **110**, 112301 (2013), URL <http://link.aps.org/doi/10.1103/PhysRevLett.110.112301>.
- [26] S. Cao, G.-Y. Qin, and S. A. Bass, *Phys.Rev.* **C88**, 044907 (2013).
- [27] P. B. Gossiaux, R. Bierkandt, and J. Aichelin, *Phys. Rev. C* **79**, 044906 (2009), URL <http://link.aps.org/doi/10.1103/PhysRevC.79.044906>.
- [28] D. Molnar, *European Physical Journal C* **49**, 181 (2006).
- [29] X. Zhu, M. Bleicher, S. Huang, K. Schweda, H. Stoecker, et al., *Phys.Lett.* **B647**, 366 (2007).
- [30] M. Nahrgang, J. Aichelin, P. B. Gossiaux, and K. Werner (2013), 1305.3823.
- [31] G. Tsileadakis, H. Appelshauser, K. Schweda, and J. Stachel, *Nucl.Phys.* **A858**, 86 (2011).